

The Complex Formation of Poly(*N*-vinylpyrrolidone) with Manganese Dodecyl Sulfate in Water Studied by ESR

Masayuki AIZAWA,* Tsuyoshi KOMATSU, and Tsurutaro NAKAGAWA

Department of Polymer Science, Faculty of Science, Hokkaido University, Sapporo 060

(Received February 4, 1982)

ESR measurements of Mn^{2+} ions in aqueous manganese dodecyl sulfate ($\text{Mn}(\text{DS})_2$) solutions with or without 0.05% poly(*N*-vinylpyrrolidone)(PVP) were carried out at 30 °C. The dependences of linewidths and of absorption intensities on the $\text{Mn}(\text{DS})_2$ concentration in ($\text{Mn}(\text{DS})_2 + 0.05\%$ PVP) solutions changed abruptly at a concentration where a PVP– $\text{Mn}(\text{DS})_2$ complex begins to form. The same dependence in $\text{Mn}(\text{DS})_2$ solutions was found around the CMC of $\text{Mn}(\text{DS})_2$ in water. From the quantitative analysis of the data obtained, it was concluded that the $\text{Mn}(\text{DS})_2$ molecules in the complex form a nearly micelle-like aggregate, and that most of Mn^{2+} ions bound onto the micelle-like aggregate or the $\text{Mn}(\text{DS})_2$ micelle exist in the Stern layer. In addition, the PVP concentration dependence of the similar quantities in ($\text{Mn}(\text{DS})_2 + \text{PVP}$) solutions with a constant $\text{Mn}(\text{DS})_2$ concentration suggested that the polymer–surfactant complex changes its structure at higher PVP concentrations.

In the past three decades, many investigators have been engaged in the study of the interaction between nonionic polymers and surfactants in water.¹⁾ By applying various types of measurements (viscosity,^{2–5)} surface tension,^{4,6,7)} solubilization,^{5–8)} electric conductivity,^{3–5)} ionic activity,^{5,9)} *etc.*^{10,11)} details of the interaction and its mechanism have become increasingly clear. One of the important observations reported so far is that a type of complex formation occurs between some polymers and surfactants; this was first suggested by the fact that the viscosity curve of some polymer solutions with surfactants resembles that of polyelectrolyte solutions.¹²⁾

Since the complex can solubilize hydrophobic compounds,^{1,8)} its structure was presumed to have a hydrophobic region. The most acceptable structural model at present^{1,7,9,10)} has surfactants bound onto a polymer to form a micelle-like structure. The full description of the structure, however, has not yet been achieved completely. Several problems remain to be solved: the number of surfactant ions in one micelle-like aggregate,¹⁰⁾ the degree of dissociation of the counterions from the complex,⁵⁾ the binding mode of the polymer to the surfactants which constitute the micelle-like aggregate.¹¹⁾

Recently, magnetic resonance methods have been widely applied to study micellar solutions.²³⁾ For example, the binding manner of ions to a micellar surface has been studied by the ESR measurement of manganese(II) ions (Mn^{2+} ions) introduced as counterions^{13–15)} or probe-ions¹⁶⁾ into micellar solutions. This method can yield information on the hydrophilic region of micelles in contrast with the spin-probe or spin-label method with nitroxide radicals which gives mainly information on the hydrophobic region of the micelles. If one uses surfactants which contain Mn^{2+} ions as counterions, this method is free from disturbing the system under investigation. In addition, ESR measurements by this method can easily be applied to systems with lower sample concentrations. In contrast, the NMR method requires a higher concentration owing to its lower sensitivity.¹¹⁾

The aim of the present paper is to investigate the behavior of Mn^{2+} ions in (polymer+surfactant) solutions by the ESR method to clarify the binding state

of Mn^{2+} ions in the polymer–surfactant complex in comparison with the behavior of Mn^{2+} ions in $\text{Mn}(\text{DS})_2$ solutions. In order to obtain the degree of dissociation of Mn^{2+} ions from the complex, absorption intensities of ESR signals will be measured. Line-widths of ESR signals will also be measured so as to establish the binding state of Mn^{2+} ions in the complex.

Experimental

Manganese dodecyl sulfate ($\text{Mn}(\text{DS})_2$) was synthesized from commercial sodium dodecyl sulfate of specially prepared reagent grade and manganese chloride of guaranteed reagent grade according to Miyamoto's method.¹⁷⁾ The $\text{Mn}(\text{DS})_2$ was purified by several recrystallization from water.

Poly(*N*-vinylpyrrolidone)(PVP) which was purchased from Nakarai Chemicals Ltd. was purified by dialysis using cellophane tubing.

Surface tension measurements by a capillary rise method were carried out at 25 ± 0.05 °C to ascertain the purity of $\text{Mn}(\text{DS})_2$ and the existence of the interaction between PVP and $\text{Mn}(\text{DS})_2$ in water.

The ESR spectra were recorded at 30 ± 0.5 °C on a JEOL model FEIX spectrometer equipped with a variable temperature accessory.

The ESR signal of solid DPPH was used as an external reference in the calculation of the absorption intensities of Mn^{2+} ions in a series of sample solutions.

Results and Discussion

In Fig. 1, the values of the surface tension of aqueous $\text{Mn}(\text{DS})_2$ solutions are plotted against the molar concentration of $\text{Mn}(\text{DS})_2$, m . Obviously there is no minimum in the resultant curve. From the break point on its curve, the value of the CMC of $\text{Mn}(\text{DS})_2$ in water was estimated to be 1.4 mmol kg^{-1} which is slightly higher than that reported in the literature.¹⁸⁾

A similar plot of aqueous ($\text{Mn}(\text{DS})_2 + 0.05\%$ PVP) solutions is also illustrated in Fig. 1; in this case, m is the number of moles of $\text{Mn}(\text{DS})_2$ per kilogram of a 0.05% aqueous PVP solution. This plot is evidently different from that of aqueous $\text{Mn}(\text{DS})_2$ solutions. It has two break points whose concentrations do not coincide with the CMC of $\text{Mn}(\text{DS})_2$ in water. This fact indicates that $\text{Mn}(\text{DS})_2$ interacts with PVP

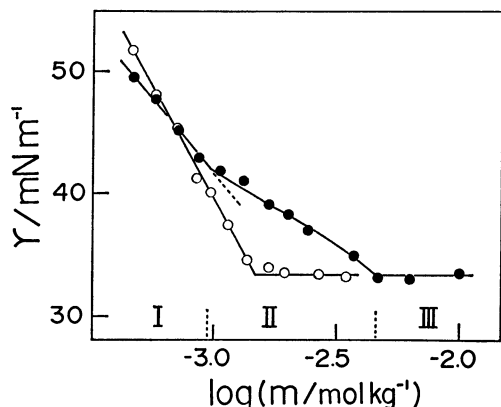


Fig. 1. Surface tension *vs.* $\log(m/\text{mol kg}^{-1})$.
○: $\text{Mn}(\text{DS})_2$ solutions, ●: $(\text{Mn}(\text{DS})_2 + 0.05\% \text{ PVP})$ solutions.

in some manner.

If one interprets the two break points according to the previous studies on the interaction between sodium dodecyl sulfate and some nonionic polymers,^{4,7} a kind of complex formation between $\text{Mn}(\text{DS})_2$ and PVP starts at the concentration of the lower break point, m_1 , and continues to the concentration of the higher one, m_2 . Above m_2 , micelles of $\text{Mn}(\text{DS})_2$ are produced in the solution without further complex formation. Thus, chemical species in the solution vary with m in the following way: in region I ($m < m_1$), Mn^{2+} ions and dodecyl sulfate ions (DS^- ions); in region II ($m_1 \leq m < m_2$), Mn^{2+} ions, DS^- ions, and complexes formed between PVP and $\text{Mn}(\text{DS})_2$ (P-S complexes); in region III ($m_2 < m$), Mn^{2+} ions, DS^- ions, P-S complexes, and $\text{Mn}(\text{DS})_2$ micelles. These three concentration regions are indicated by roman numerals above the abscissa in the figure.

ESR spectra of Mn^{2+} ions ($S=5/2$ and $I=5/2$) obtained in the present study were composed of six unequivalent lines; each of which contains five unresolved lines. Since the fourth line from the low field side is nearly Lorentzian, its linewidths and absorption intensities were measured as a function of m .

Figure 2(a) shows the dependence of the peak-to-peak linewidth, W_{pp} , on m in two systems; the one is aqueous $\text{Mn}(\text{DS})_2$ solutions, and the other is aqueous $(\text{Mn}(\text{DS})_2 + 0.05\% \text{ PVP})$ solutions. In appearance, there is little difference between the two systems; W_{pp} is nearly constant to $m \approx 1 \text{ mmol kg}^{-1}$, and then increases with m . Since this concentration approximately corresponds to the CMC of $\text{Mn}(\text{DS})_2$ in water or to the concentration, m_1 , at which the P-S complex begins to form in the $(\text{Mn}(\text{DS})_2 + 0.05\% \text{ PVP})$ solutions, the increase in W_{pp} reflects the formation of micelles or P-S complexes.

According to Garrett and Morgan,¹⁹ the broadening of W_{pp} of Mn^{2+} complexes in solutions is caused by the decrease in perturbational correlation time and/or by the alteration in the time-dependent spin Hamiltonian of Mn^{2+} ions. When Mn^{2+} ions are bound onto the surface of the micelle-like region, both effects can be expected to occur.

The similarity of the W_{pp} - m plot between the two

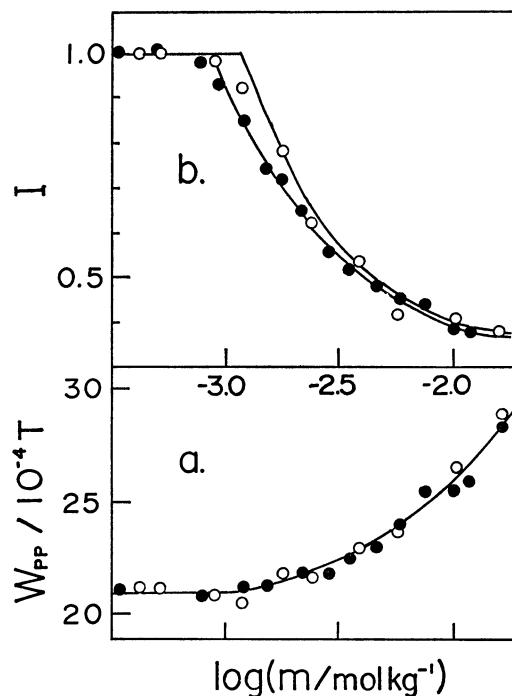


Fig. 2. (a) Linewidth *vs.* $\log(m/\text{mol kg}^{-1})$. (b) Normalized intensity *vs.* $\log(m/\text{mol kg}^{-1})$. ○: $\text{Mn}(\text{DS})_2$ solutions, ●: $(\text{Mn}(\text{DS})_2 + 0.05\% \text{ PVP})$ solutions.

systems, therefore, may imply that there is little difference in the binding state of Mn^{2+} ions; it suggests that $\text{Mn}(\text{DS})_2$ molecules bound onto the PVP aggregate to form a micelle-like structure.

Normalized absorption intensities, I , of Mn^{2+} ions in the two systems are shown as a function of m in Fig. 2(b); here, I was obtained by the normalization of values which resulted from dividing absorption intensities, I_A , by m . The I_A was calculated through the following relation which holds for Lorentzian line shapes:

$$I_A \propto h_{pp} \times W_{pp}^2, \quad (1)$$

where h_{pp} is the peak-to-peak height.

A small difference in the behavior of the I - m curve can be seen between the two systems owing to the rate of change in I being greater than that in W_{pp} . In the case of $\text{Mn}(\text{DS})_2$ solutions, I takes a constant value ($=1.0$) below $m=1.1 \text{ mmol kg}^{-1}$ which is nearly equal to the CMC, and then decreases steeply to a saturation value (≈ 0.35). On the other hand, in the case of $(\text{Mn}(\text{DS})_2 + 0.05\% \text{ PVP})$ solutions, the steep decrease in I begins at $m=0.94 \text{ mmol kg}^{-1}$ which is approximately equal to m_1 in Fig. 1. At higher concentrations, the I - m curve approaches gradually to that of $\text{Mn}(\text{DS})_2$ solutions.

According to the previous ESR studies on Mn^{2+} complexes in solutions,^{20,21} the loss of signal intensity of Mn^{2+} ions is attributed to the extreme broadening of the linewidths beyond detection. This broadening is caused by a large distortion from the octahedral symmetry of $\text{Mn}(\text{H}_2\text{O})_6^{2+}$ on the formation of unsymmetrical inner-sphere complexes.

If one considers, on the basis of a simple micellar model, that Mn^{2+} ions in $\text{Mn}(\text{DS})_2$ micellar solutions

exist in three regions; the Stern layer, the diffuse layer, and the bulk water, Mn^{2+} ions "bound" onto the micelles are those in the two layers. Since Mn^{2+} ions in the Stern layer form inner-sphere complexes with DS^- ions constituting micelles, they are responsible for the intensity loss. On the other hand, those in the diffuse layer which form outer-sphere complexes with the DS^- ions contribute to the broadening of linewidths in Fig. 2(a).

By analyzing the intensity loss in Fig. 2(b) on the basis of the simple idea, one can proceed to a quantitative discussion.

Denoting the degree of dissociation of Mn^{2+} ions from $\text{Mn}(\text{DS})_2$ micelles by α , and the fraction of Mn^{2+} ions in the diffuse layer in total Mn^{2+} ions bound onto micelles by β , I_A is combined with α and β by the following relation;

$$I_A \propto m_f + \alpha(m - m_f) + \beta(1 - \alpha)(m - m_f), \quad (2)$$

where m_f is the concentration of free $\text{Mn}(\text{DS})_2$ being in equilibrium with the $\text{Mn}(\text{DS})_2$ in a micellar state. The second and the third term represent the contribution from Mn^{2+} ions dissociating from micelles and those in the diffuse layer, respectively.

Dividing the right hand side of Eq. 2 by m , I is derived as follows:

$$\begin{aligned} I &= \frac{m_f}{m} + \alpha\left(1 - \frac{m_f}{m}\right) + \beta(1 - \alpha)\left(1 - \frac{m_f}{m}\right) \\ &= (1 - \alpha - \beta + \alpha\beta)\frac{m_f}{m} + \alpha + \beta - \alpha\beta. \end{aligned} \quad (3)$$

Moreover, by simple transformation of Eq. 3, the following equation is obtained;

$$m(1 - I) = (\alpha\beta + 1 - \alpha - \beta)(m - m_f). \quad (4)$$

Supposing that $\text{Mn}(\text{DS})_2$ molecules bound onto PVP form a micelle-like aggregate, in the case of $(\text{Mn}(\text{DS})_2 + 0.05\% \text{ PVP})$ solutions, the equations similar to Eqs. 3 and 4 can be described as follows:

$$I = (1 - \alpha^p - \beta^p + \alpha^p\beta^p)\frac{m_f^p}{m} + \alpha^p + \beta^p - \alpha^p\beta^p, \quad (5)$$

$$m(1 - I) = (\alpha^p\beta^p + 1 - \alpha^p - \beta^p)(m - m_f^p), \quad (6)$$

where α^p , β^p , and m_f^p are the corresponding quantities to α , β , and m_f in Eqs. 3 and 4.

Plots of I vs. m_f/m and I vs. m_f^p/m based on Eqs. 3 and 5 respectively are shown in Fig. 3. Here, the concentrations at the break points in Fig. 2(b) were used as the constant values of m_f and m_f^p ; that is, $m_f = 1.1 \text{ mmol kg}^{-1}$ and $m_f^p = 0.9_4 \text{ mmol kg}^{-1}$. In the strict sense, m_f^p varies from $0.9_4 \text{ mmol kg}^{-1}$ to 1.1 mmol kg^{-1} in region II with an increase in m . The present assumption that m_f^p takes a constant value of $0.9_4 \text{ mmol kg}^{-1}$, however, does not introduce serious errors in the calculation of m_f^p/m in Eq. 5 and $(m - m_f^p)$ in Eq. 6, since the difference between the two values of m_f^p ($=0.1_6 \text{ mmol kg}^{-1}$) is much smaller than the value of m_2 ($=4.6 \text{ mmol kg}^{-1}$); the errors become largest at m_2 . Roman numerals above the abscissa indicate the regions corresponding to the three concentration regions in Fig. 1. The two plots in the figure are depicted by the same straight line in regions II and III; in the plot of I vs. m_f^p/m , there is no in-

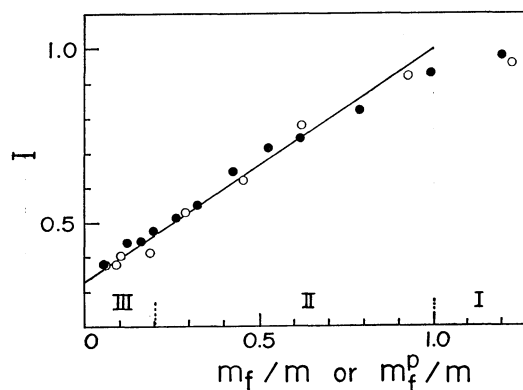


Fig. 3. Plots of I in $\text{Mn}(\text{DS})_2$ solutions vs. m_f/m : (O), and I in $(\text{Mn}(\text{DS})_2 + 0.05\% \text{ PVP})$ solutions vs. m_f^p/m : (●).

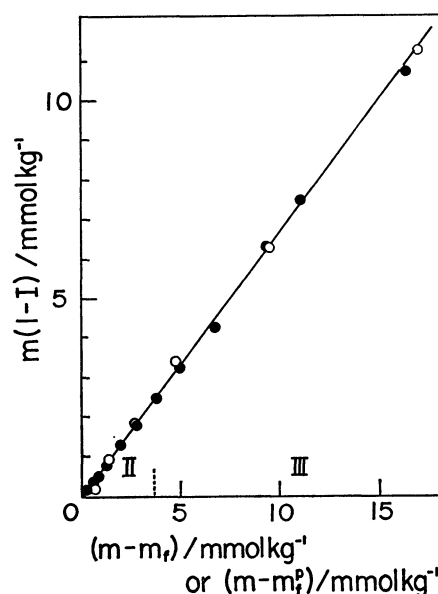


Fig. 4. Plots of $m(1 - I)$ in $\text{Mn}(\text{DS})_2$ solutions vs. $(m - m_f)$: (O), and $m(1 - I)$ in $(\text{Mn}(\text{DS})_2 + 0.05\% \text{ PVP})$ solutions vs. $(m - m_f^p)$: (●).

flexion at the boundary between region II and region III.

Similarly, plots of $m(1 - I)$ vs. $(m - m_f)$ and $m(1 - I)$ vs. $(m - m_f^p)$ based on Eqs. 4 and 6 respectively are shown in Fig. 4. The two plots are evidently on the same line with no inflection in regions II and III as well as in Fig. 3.

Thus, the results obtained in Figs. 3 and 4 indicate that $\alpha \approx \alpha^p$ and $\beta \approx \beta^p$; in other words, the binding manner of Mn^{2+} ions onto the micelle-like aggregate is similar to that of Mn^{2+} ions onto the $\text{Mn}(\text{DS})_2$ micelles.

From the dependence of m_1 or CMC on the hydrocarbon chain length of surfactants, Arai and coworkers⁷⁾ have reported that the free energy of transferring a CH_2 from aqueous solution to the micelle-like aggregate in the P-S complex agrees with the result in the simple micellar solutions without added polymers. It can, therefore, be supposed that the structure of this micelle-like aggregate is almost identical with that

of an ordinary micelle.

It is clear from Eqs. 3 and 4, that the simultaneous determination of α and β from the y -intercept and the slope of the straight lines (Figs. 3 and 4) is impossible; the value of β was therefore estimated by the use of a value for α reported by Satake and co-workers.²²⁾ From electric conductivity data, they estimated α of magnesium dodecyl sulfate ($\text{Mg}(\text{DS})_2$) micelles to be 0.21 in a $0.1 \text{ mol dm}^{-3} \text{ MgSO}_4$ solution.

The use of this value for $\text{Mn}(\text{DS})_2$ micelles in the present study is permissible for the following two reasons; one is the similar chemical character of Mn^{2+} ions and Mg^{2+} ions,²⁴⁾ and the other is the weak effect of added electrolytes on the aggregation number of dodecyl sulfate ions in micelles of bivalent metal dodecyl sulfates.²²⁾

Substituting this value ($=0.21$) for α in the following equation which is obtained by analysis of the lines in Figs. 3 and 4:

$$\alpha + \beta - \alpha\beta = 0.32, \quad (7)$$

the value of β is estimated to be 0.14.

The magnitude of this β value implies that most of Mn^{2+} ions bound onto micelles exist in the Stern layer as inner-sphere complexes with DS^- ions. Since β^p is nearly equal to β , the same conclusion can also be derived in the case of the micelle-like aggregate in P-S complexes.

In order to investigate whether the structures of P-S complexes change or not with an increase in the PVP concentration, the linewidths and relative intensities of the ESR signal of Mn^{2+} ions in $(\text{Mn}(\text{DS})_2 + \text{PVP})$ solutions with various amounts of PVP were measured at a constant $\text{Mn}(\text{DS})_2$ concentration.

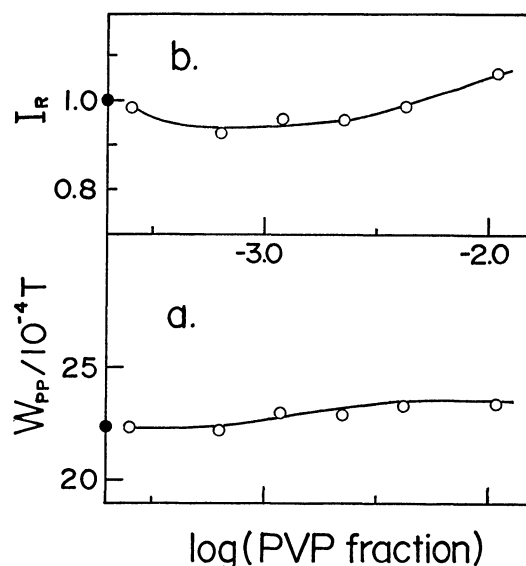


Fig. 5. (a) Linewidth vs. log(weight fraction of PVP). (b) Relative intensity vs. log(weight fraction of PVP). $\text{Mn}(\text{DS})_2$ concentration $= 3.21 \text{ mmol kg}^{-1}$. Closed circles represent the values of the $\text{Mn}(\text{DS})_2$ solution without PVP.

If the structure assumed for the complexes in the above discussion remains unchanged with increase in the PVP concentration, W_{pp} will increase slightly, whereas I will decrease asymptotically, for the concentration m_1 gradually decreases with the increase in the PVP concentration.¹¹⁾

The results where $m = 3.21 \text{ mmol kg}^{-1}$ are shown as a function of the weight fraction of PVP in Fig. 5; the relative intensity, I_R , means the ratio of I_A in $(\text{Mn}(\text{DS})_2 + \text{PVP})$ solutions to that in the $\text{Mn}(\text{DS})_2$ solutions without PVP. Obviously, the curves depicted in the figure are not the predicted ones. W_{pp} in Fig. 5(a) is nearly constant below 0.2%, and then increases slightly, while I_R decreases asymptotically to 0.2%, but above that concentration it increases evidently.

This behavior may suggest a structural change of the P-S complex at higher PVP concentrations; the structure may transform into one with a weak binding potential for Mn^{2+} ions.

References

- 1) S. Saito, *Yukagaku*, **12**, 133 (1963).
- 2) T. Isemura and A. Imanishi, *J. Polym. Sci.*, **33**, 337 (1958).
- 3) S. Harada, T. Komatsu, and T. Nakagawa, *Nippon Kagaku Kaishi*, **1974**, 622.
- 4) M. N. Jones, *J. Colloid Interface Sci.*, **23**, 36 (1967).
- 5) N. Murai, S. Makino, and S. Sugai, *J. Colloid Interface Sci.*, **41**, 399 (1972).
- 6) M. J. Schwuger, *J. Colloid Interface Sci.*, **43**, 491 (1973).
- 7) H. Arai, M. Murata, and K. Shinoda, *J. Colloid Interface Sci.*, **37**, 223 (1971).
- 8) F. Tokiwa and K. Tsujii, *Bull. Chem. Soc. Jpn.*, **46**, 2684 (1973).
- 9) M. Nakagaki and S. Shimabayashi, *Nippon Kagaku Kaishi*, **1972**, 989.
- 10) K. Shirahama, *Colloid Polym. Sci.*, **252**, 978 (1974).
- 11) B. Cabane, *J. Phys. Chem.*, **81**, 1639 (1977).
- 12) S. Saito, *Kolloid-Z.*, **133**, 12 (1953).
- 13) J. Oakes, *J. Chem. Soc., Faraday Trans. 2*, **69**, 1321 (1973).
- 14) A. Kitahara, O. Ohashi, and K. Kon-no, *J. Colloid Interface Sci.*, **49**, 108 (1974).
- 15) M. Ueki and Y. Uzu, *Bull. Chem. Soc. Jpn.*, **53**, 1445 (1980).
- 16) A. Hasegawa, Y. Michihara, and M. Miura, *Bull. Chem. Soc. Jpn.*, **43**, 3116 (1970).
- 17) S. Miyamoto, *Bull. Chem. Soc. Jpn.*, **33**, 371 (1960).
- 18) S. Miyamoto, *Bull. Chem. Soc. Jpn.*, **33**, 375 (1960).
- 19) B. B. Garrett and L. O. Morgan, *J. Chem. Phys.*, **44**, 890 (1966).
- 20) L. Burlamacchi and E. Tiezzi, *J. Phys. Chem.*, **73**, 1588 (1969).
- 21) L. Burlamacchi, G. Martini, and M. Romanelli, *J. Chem. Phys.*, **59**, 3008 (1973).
- 22) I. Satake, I. Iwamatsu, S. Hosokawa, and R. Matuura, *Bull. Chem. Soc. Jpn.*, **36**, 204 (1963).
- 23) H. Wennerström and B. Lindman, *Phys. Rep.*, **52**, 33 (1979).
- 24) G. Anderegg, *Helv. Chim. Acta*, **43**, 414 (1960).